Compromised GABAergic inhibition contributes to tumor-associated epilepsy

Georgina MacKenzie[a,1], **Kate K. O'Toole**[b,1], **Stephen J. Moss**[a], and **Jamie Maguire, Ph.D.**[a,*] **[Assistant Professor]**

[a]Department of Neuroscience, Tufts University School of Medicine, Boston, MA 02111, United States

[b]Training in Education and Critical Research Skills (TEACRS) Program, Tufts University School of Medicine, Boston, MA 02111, United States

Abstract

Glioblastoma Multiforme (GBM) is the most common form of primary brain tumor with 30–50% of patients presenting with epilepsy. These tumor-associated seizures are often resistant to traditional antiepileptic drug treatment and persist after tumor resection. This suggests that changes in the peritumoral tissue underpin epileptogenesis. It is known that glioma cells extrude pathological concentrations of glutamate which is thought to play a role in tumor progression and the development of epilepsy. Given that pathological concentrations of glutamate have been shown to dephosphorylate and downregulate the potassium chloride cotransporter KCC2, we hypothesized that glioma-induced alterations in KCC2 in the peritumoral region may play a role in tumor-associated epilepsy. Consistent with this hypothesis, we observe a decrease in total KCC2 expression and a dephosphorylation of KCC2 at residue Ser940 in a glioma model which exhibits hyperexcitability and the development of spontaneous seizures. To determine whether the reduction of KCC2 could potentially contribute to tumor-associated epilepsy, we generated mice with a focal knockdown of KCC2 by injecting AAV2-Cre-GFP into the cortex of floxed KCC2 mice. The AAV2-Cre-mediated knockdown of KCC2 was sufficient to induce the development of spontaneous seizures. Further, blocking NKCC1 with bumetanide to offset the loss of KCC2 reduced the seizure susceptibility in glioma-implanted mice. These findings support a mechanism of tumor-associated epilepsy involving downregulation of KCC2 in the peritumoral region leading to compromised GABAergic inhibition and suggest that modulating chloride homeostasis may be useful for seizure control.

Keywords

Glioma; Tumor; Epilepsy; GABA; KCC2; Seizures

---

[*]Corresponding author at: Department of Neuroscience, Tufts University School of Medicine, 136 Harrison Ave., SC205 Boston, MA 02111, United States. Jamie.Maguire@tufts.edu (J. Maguire).
[1]These authors contributed equally to the work.

1. Introduction

Gliomas are the most common form of primary brain tumor and frequently present with seizures (Iuchi et al., 2015; Kerkhof and Vecht, 2013; van Breemen et al., 2007). The tumor mass itself does not show epileptiform activity, but rather seizures originate from neurons in the peritumoral region (Kohling et al., 2006; Patt et al., 2000; Senner et al., 2003). The standard treatment for glioma involves surgical resection; however, tumor associated epilepsy often persists following glioma removal (Iuchi et al., 2015). Prognosis of glioma patients is poor and is exacerbated by the associated seizures which are often refractory to traditional anti-epileptic drugs (AED) (de Groot et al., 2012; Iuchi et al., 2015) worsening treatment outcomes and palliative care. The underlying mechanisms driving the epileptogenic process remain unclear; however, an improved understanding of the pathophysiological process occurring in the peritumoral region is essential for effective seizure management.

Elevated glutamate concentrations in the extracellular space surrounding gliomas has been observed in both human patients and in rodent glioma models (Buckingham et al., 2011; Marcus et al., 2009) and is associated with a higher risk of seizures (Yuen et al., 2012). Elevated glutamate concentrations associated with gliomas are thought to be due to the reduced expression of the glutamate transporter EAAT2 (GLT-1) (de Groot et al., 2005; Ye et al., 1999; Yuen et al., 2012) and increased expression of the cysteine-glutamate exchange system x_c^- (Ye et al., 1999; Yuen et al., 2012) which import and export glutamate across the cell membrane respectively. The extracellular glutamate concentration reaches excitotoxic levels in the immediate tumor invasion zone, resulting in neuronal cell death and the creation of space for tumor migration and expansion (Ye and Sontheimer, 1999). The spillover of glutamate into the peritumoral tissue has been proposed to increase neuronal excitability and generate epileptiform activity (Buckingham et al., 2011). Brain slices generated from tumor bearing rodents show elevated glutamate release (Behrens et al., 2000; Buckingham et al., 2011) and hyperexcitability in the peritumoral region (Kohling et al., 2006; Patt et al., 2000; Senner et al., 2003) which could be reduced but not completely blocked by preventing glutamate export through system x_c^- with sulfasalazine (SAS) (Buckingham et al., 2011; Campbell et al., 2012).

In addition to increased excitatory signaling, which will have a significant influence on the activation threshold of peritumoral neurons, changes in inhibitory GABA(A) receptor signaling have also been implicated in the pathology of tumor-associated epilepsy (Conti et al., 2011; Pallud et al., 2013). The inhibitory actions of GABA in the mature brain are dependent upon the potassium chloride co-transporter KCC2 which, by extruding chloride from the cell, maintains the GABA reversal potential (E_{GABA}) at potentials equal to or more negative than the resting membrane potential (Payne et al., 2003; Rivera et al., 1999). The actions of KCC2 are opposed by the sodium potassium chloride co-transporter NKCC1 which transports chloride into the cell. The increased NKCC1:KCC2 ratio is responsible for the excitatory actions of GABA during normal development (Ben-Ari, 2002). Alterations in the expression of these transporters have also been demonstrated under pathological conditions and implicated in numerous neurological disorders, including epilepsy (Barmashenko et al., 2011; Huberfeld et al., 2007; Pathak et al., 2007). The downregulation

of KCC2 expression and reduced chloride extrusion capacity leads to a depolarizing shift in E_{GABA} and a switch from hyperpolarizing to depolarizing and even excitatory $GABA_A$ receptor signaling (Hewitt et al., 2009; Huberfeld et al., 2007; O'Toole et al., 2013; Sarkar et al., 2011). Recently changes in cation-cotransporter expression have been shown in the peritumoral region of human glioma patients (Aronica et al., 2007; Conti et al., 2011; Pallud et al., 2013) resulting in a depolarizing shift in the GABA reversal potential (Conti et al., 2011). Similarly, a reduction in KCC2 expression has been observed in the peritumoral region in a mouse glioma model and has been proposed to contribute to tumor-associated epilepsy (Campbell et al., 2015).

The expression of chloride cation cotransporters is tightly regulated by changes in phosphorylation state (Kahle and Delpire, 2016; Kahle et al., 2013; Lee et al., 2007; Lee et al., 2010). It has been shown that phosphorylation of KCC2 residue serine 940 (Ser940) is important for the cell surface stability and pumping efficiency of the transporter (Lee et al., 2007). Dephosphorylation of Ser940 occurs through an NMDA and protein phosphatase 1 (PP1) dependent process in response to pathological levels of glutamate (Lee et al., 2011) such as observed in glioma cells (Marcus et al., 2009). Dephosphorylation of KCC2 at residue Ser940 has been shown to result in a downregulation of KCC2, a collapse of the chloride gradient, and a depolarizing shift in E_{GABA} (Lee et al., 2011; MacKenzie and Maguire, 2015; O'Toole et al., 2013; Sarkar et al., 2011). Given that pathological concentrations of glutamate have been measured in peritumoral tissue (Marcus et al., 2009) and the role of glutamate in the regulation of KCC2 (Lee et al., 2011), we hypothesized that glutamate release from glioma cells may promote the dephosphorylation of KCC2 residue ser940 and alter KCC2 expression in the peritumoral region and contribute to tumor-associated epilepsy.

In this study we demonstrate a significant reduction in the phosphorylation of KCC2 at residue Ser940 and a downregulation of KCC2 in the peritumoral region in a mouse glioma model associated with neuronal hyperexcitability and the development of spontaneous seizures. Using AAV-Cre injections into the cortex of floxed KCC2 mice, we demonstrated that a comparable localized loss of KCC2 is sufficient to induce spontaneous seizures. Further, we demonstrated that the tumor-associated seizure susceptibility could be controlled with the NKCC1 inhibitor bumetanide, a loop diuretic which has been shown to restore E_{GABA} to more hyperpolarized potentials (for review see (Kahle et al., 2008)). These data support the role of KCC2 in contributing to the development of tumor-associated epilepsy, provide novel mechanistic insights into how gliomas modulate transporter function, and highlight the potential of targeting cation-chloride cotransporters for seizure management.

2. Methods

2.1. Animal handling

Adult (3-month-old), male nude mice, C57Bl/6 mice, and S940A floxed KCC2 mice (Silayeva et al., 2015) were housed at the Tufts University School of Medicine, Division of Laboratory Animal Medicine. Mice were housed in clear plastic cages (5 mice/cage) in a temperature- and humidity-controlled environment with a 12 h light/dark cycle (light on at 7:00 a.m.) and ad libitum access to food and water. Nude mice were housed under sterile

housing conditions. Animals were handled according to protocols approved by the Tufts University Institutional Animal Care and Use Committee.

2.2. Cell culture

Rat-derived glioma C6 cells (ATCC: CCL-107, Lot #59673008) were maintained at 37°C and 5% CO2, in Dulbecco's Modification of Eagle's Medium (DMEM; Cellgro) supplemented with 10% FBS (Hyclone). Cells were grown in large volume T150 flasks and passaged regularly with trypsin to prevent growth beyond a confluent monolayer. To determine levels of glutamate extrusion, cells were plated in 12 well plates using FluroBrite™ DMEM (Gibco) and grown to 80% confluency. Media samples were assayed for Glutamate concentration using the Amplex® Red Kit (Invitrogen) according to manufacturer's specifications.

2.3. Glioma model

Adult (10–12 weeks of age) male nude mice were anesthetized with 100 mg/kg ketamine and 10 mg/kg xylazine until unresponsive to a foot pinch. A lengthwise incision was made along the scalp to expose the skull. To implant the glioma cells, a small burr hole was made over the right motor cortex (M1 coordinates: +0.8 mm anterior/posterior, ±1.0 mm medial/lateral, −1.0 mm dorsal/ventral) and a 5 μl Hamilton syringe was used to slowly inject 5 μl of either vehicle or C6 cell suspension (100,000 cells). This model established a glioma, largely confined to the cortex, which increased in size over two weeks following implantation (Fig. 1a–b).

2.4. Electrophysiology slice preparation

Sham- or glioma-implanted animals were anesthetized with isoflurane, decapitated, and the brain rapidly removed. Coronal sections, 350 μm thick were prepared in ice-cold ACSF using a Leica vibratome. The slices were stored oxygenated at 34 °C for at least 1 h before recording. Hemislices containing tumor tissue or the sham injection tract (ipsilateral) or matched contralateral hemislices were placed into a recording chamber maintained at 34 °C and perfused with normal ACSF containing: 126 mM NaCl, 26 mM NaHCO3, 1.25 mM NaH2PO4, 2.5 mM KCl, 2 mM CaCl2, 2 mM MgCl2, and 10 mM dextrose (300–310 mOsm). Adequate O2 tension and physiological pH (~7.4) was maintained by continually bubbling the media with a gas mixture: 95% O2/5% CO2.

2.5. Gramicidin perforated patch clamp recording

Perforated patch clamp recordings were performed as previously described (MacKenzie and Maguire, 2015; O'Toole et al., 2013; Sarkar et al., 2011) using glass micropipettes with DC resistance of 5–8 MΩ backfilled with internal solution containing (in mM): 130 K-gluconate, 10 KCl, 4 NaCl, 10 HEPES, 0.1 EGTA, 2 Mg-ATP, 0.3 Na-GTP (pH = 7.25, 280–290 mOsm/LH$_2$O) with 50 μg/ml gramicidin (ABCD, Sigma). Upon generating a high resistance seal (>1 GΩ), perforation was determined by the decrease in membrane resistance, which dropped below 200 MΩ within approximately 20 min following patch formation as described previously (O'Toole et al., 2013; Sarkar et al., 2011), an increase in capacitive transients in response to a −5 mV voltage step, and V$_{pipette}$ reached a value close to the

RMP. No significant difference in series resistance was observed between experimental groups. Series resistance and capacitive transients were periodically monitored throughout the experiment and data were immediately rejected if the resistance suddenly dropped and/or the membrane potential suddenly changed, indicating rupture of the patch (Yu et al., 2013).

2.6. Input-output experiments

Field potentials were evoked by stimulation at 0.05 Hz within the superficial layers of the cortex (III or IV) and responses were recorded in layer V/VI. Bipolar electrodes were used to deliver a constant-current stimulus. The stimulus intensity was determined by recording a threshold response at a width (W) of 60 μs with no response at 20 μs. The W of the stimulus was increased stepwise by 20 μs to create I/O curves ranging from 20 to 240 μs. Four population field EPSPs (fEPSPs) were recorded at each W, and the maximum slope of the responses (volts per second) was measured over a 1–3 ms window of the fEPSP rising phase. Due to the biphasic nature of the fEPSP responses, the slope of the rising phase was measured over 1–5 ms of the fEPSP measured from the source (upward). Population spikes were excluded from the measurements of the slope of the fEPSP. The average slope was calculated for each stimulus and the average was calculated over the 4 fEPSPs recorded at each stimulation width. Input/output curves were fit with a Boltzman equation using OriginLab software: $y = (MIN-MAX)/(1 + \exp((x - x_0)/dx)) + MAX$), where x_0 is the y value halfway between the two limiting values MIN and MAX and therefore represents the half maximum stimulus width (W50). MIN is the minimum response elicited by the lowest stimulus width (20 μs), MAX is the maximum response elicited by the largest stimulus width (240 μs), dx is a slope factor (OriginLab).

2.7. In vitro epileptiform activity

Spontaneous extracellular field potentials were measured in layer V/VI of the cortex nearest the edge of the tumor in ipsilateral slices and in mirror sites within contralateral slices. Synchronous discharges were recorded in increasing concentrations of extracellular KCl, normal ACSF (2.5), 5.0, 7.5, and 10 mM. Only slices that exhibited synchronous discharges in 10 mM KCl were considered to have a sufficiently healthy local circuitry to be included in the data analysis. Epileptiform discharges were considered to be paroxysmal field potentials that had increased amplitude 2 times the standard deviation above the baseline activity recorded in nACSF.

2.8. Electroencephalogram (EEG) recording

EEG recordings and analysis were performed as previously described (Lee and Maguire, 2013; O'Toole et al., 2013). Mice were anesthetized with 100 mg/kg ketamine and 10 mg/kg xylazine until unresponsive to a foot pinch. A lengthwise incision was made along the scalp and a pre-fabricated headmount (Pinnacle Technology, part #8201) was fixed to the skull with four screws, which serve as differential recording leads. The headmount was fixed to the skull using dental cement and the animal was allowed to recover for a minimum of 5 days prior to experimentation. Electroencephalogram recordings were collected using a 100× gain preamplifier high pass filtered at 1.0 Hz (Pinnacle Technology, part #8202-SE) and tethered turnkey system (Pinnacle Technology, part #8200). Spontaneous seizures were assessed using 24/7 EEG recording for 3 weeks. Seizure susceptibility was determined by

measuring EEG recordings for two hours post kainic acid (10 mg/kg) administration. Seizure events were identified by the sudden onset of high amplitude activity, at least 2.5 times the standard deviation of the baseline and lasting longer than 5 s in duration. Seizure activity was also identified by consistent changes in the Power of the fast Fourier transform of the EEG, including a change in the Power and the frequency of activity over the course of the event. Abnormal periods of EEG activity which cannot be defined as a seizure, including periods of rhythmic spiking lasting longer than 30 s, along with ictal events were defined as "epileptiform activity". These criteria have been used previously by our group (Lee and Maguire, 2013; O'Toole et al., 2013) as well as by other experts in the field (Castro et al., 2012). Seizure latency was defined as the time elapsed from the injection of kainic acid to the start of the first electrographic seizure. The number and duration of individual epileptiform events were calculated.

2.9. Western blot

Western blot analysis was performed as previously described (MacKenzie and Maguire, 2015; O'Toole et al., 2013; Sarkar et al., 2011). Two weeks following glioma-implantation, animals were anesthetized with isoflurane then killed by decapitation. The ipsilateral cortex lateral and posterior to the surface of the tumor and the contralateral cortex of matching location and surface area were rapidly dissected out and placed in ice-cold homogenization buffer [containing (in mM): 10 NaPO4, 100 NaCl, 10 sodium pyrophosphate, 25 NaF, 5 EDTA, 5 EGTA, 2% Triton X-100, 0.5% deoxycholate, 1 sodium vanadate, pH 7.4 in the presence of protease inhibitors (Complete Mini, Roche, and fresh PMSF). The tissue was briefly sonicated, the lysate was incubated on ice for 30 min, and then the supernatant was collected following centrifugation at 14,000 rpm for 5 min. Protein concentrations were determined using the DC Protein Assay (Bio-Rad). Total protein (25 μg) was loaded onto a 10% SDS polyacrylamide gel, subjected to gel electrophoresis, transferred to an Immobilon-P membrane (Millipore), blocked in 10% nonfat milk, and probed with a monoclonal antibody specific for KCC2 (1:1000, Millipore), or Ser940 (1:1000, a generous gift from Dr. Steve Moss). The blots were incubated with peroxidase-labeled anti-rabbit IgG (1:2000, GE Healthcare) and immunoreactive proteins were visualized using enhanced chemiluminescence (GE Healthcare). Optical density measurements were determined using NIH ImageJ software.

2.10. KCC2 knockdown

A model of KCC2 knockdown in the cortex was established by injecting AAV2-Cre-GFP (Vector BioLabs, #7016) into the cortex of floxed KCC2 mice (a generous gift from Dr. Steve Moss; previously published in (Silayeva et al., 2015)). A small burr hole was made as described above and a 5 μl Hamilton syringe was used to slowly inject 1 μl of either AAV-Cre or AAV-GFP into M1 of floxed KCC2 transgenic mice. Control animals underwent the same surgery, but received an injection of AAV-GFP (Vector BioLabs, #7004). Loss of KCC2 in the cortex was confirmed by Western blot analysis.

2.11. Bumetanide and sulfasalazine (SAS) treatments

To investigate the therapeutic potential of bumetanide (Sigma), micro-osmotic pumps (Alzet) were placed subcutaneously between the scapulae via the same incision described

above. Pumps were filled with 0.64 mg bumetanide in 100 μl 15% EtOH/50% DMSO/dH2O in order to deliver approximately 0.8 mg/kg/h for up to 21 days (Brandt et al., 2010). The suture site was then closed and animals were given an analgesic (0.05 mg/kg buprenorphine) and monitored post operatively for three days. Control mice underwent the same surgery and were implanted with Alzet micro-osmotic pumps containing vehicle (15% EtOH/50% DMSO/dH2O). To investigate the role of glutamate release from glioma cells in the dephosphorylation and downregulation of KCC2, mice were treated with sulfasalazine (SAS) micro-osmotic pumps (Alzet) were filled with 5 mg/ml salfasalazine 0.9% saline/1% DMSO, to continuously deliver for up to 21 days. The animals were implanted with the osmotic minipumps at the time of glioma implantation which provided continuous drug exposure until experimentation one or two weeks post implantation.

2.12. Statistical tests

Experiments involving comparison between two experimental groups (vehicle versus kainic acid; contralateral versus ipsilateral), statistical significance was determined using a Student's *t*-test. Statistical significance was determined using either a one-way ANOVA or a two-way ANOVA for experiments involving comparison of more than two experimental groups. Where appropriate a Chi Square test with contingency tables was used to compare differences between groups. All statistical tests were performed using Prism software (GraphPad). All data are represented as +/− SEM. * Denotes statistical significance of $p < 0.05$.

3. Results

3.1. Hyperexcitability and spontaneous seizures in a mouse glioma model

This study employed a mouse glioma xenograft model (Kohling et al., 2006; Senner et al., 2003) generated by implanting adult male nude mice with rat C6 glioma cells (ATCC® CCL107™) into the M1 cortex which progressively increased in mass and invaded the surrounding tissue (Fig. 1a–b). Glioma weight was 159.0 ± 1.8 mg at 1 week and 204.8 ± 18.1 mg at 2 weeks post glioma-implantation (Fig. 1b; n = 6 mice per experimental group; p < 0.05 determined using a using a one-way ANOVA.). Previously studies implicated glutamate release from glioma cells in both tumor progression and the development of tumor-associated epilepsy (de Groot and Sontheimer, 2011). To confirm that the C6 glioma cell line excretes glutamate in our hands, we measured glutamate levels in a cell culture fluometric assay. C6 cells were grown to confluence, fresh media supplemented with cysteine was added to each well and the glutamate concentration assayed at 0, 1, 3 and 6 h. The glutamate concentration in the media increased to a pathological concentration of 194.3 ± 24.7 μM within 6 h (Fig. 1c; n = 4; $p < 0.05$ determined using a repeated measures ANOVA), similar to glutamate concentrations reported in previous studies (Ye and Sontheimer, 1999) and validating the use of this glioma mouse model.

To determine whether the peritumoral tissue is also hyperexcitable as has been shown previously in human tissue and other rodent glioma models (Buckingham et al., 2011; Campbell et al., 2012; Kohling et al., 2006; Patt et al., 2000; Senner et al., 2003), we performed extracellular field recordings from acute cortical slices one week following

implantation of glioma cells. Input-output curves were generated in peritumoral cortex in response to increasing stimulus width (see Methods) and compared to the corresponding region in the control contralateral cortex. Representative fEPSPs are shown in Fig. 2. The average percent maximum slope of the fEPSP was plotted against the stimulus width to generate input-output (I/O) curves for ipsilateral (grey dots) and contralateral (black dots) cortex (Fig. 2). The I/O relationships were fitted with a Boltzmann function where W_{50} is the stimulus intensity that generates the half maximal response and k is the slope factor. We observe a leftward shift in the I/O curve in the ipsilateral cortex ($W_{50} = 90.8 \pm 4.82$ μs; $k = 35.7 \pm 3.84$) compared to the contralateral control slices ($W_{50} = 114.3 \pm 5.51$ μs; $k = 44.3 \pm 3.16$) with no change in slope (Fig. 2; n = 10 slices, 3–4 mice per experimental group; p < 0.05 determined using a Student's t-test). This leftward shift in the I/O curves in the ipsilateral cortex surrounding the glioma suggests increased excitability of the peritumoral tissue.

To determine whether the increased neuronal excitability in the ipsilateral cortex translated to an increase in epileptiform activity, epileptiform activity in response to incremental increases in extracellular KCl in the contralateral and ipsilateral cortices was recorded. Acute slices were generated from sham-or glioma-implanted animals at 1 or 2 weeks post implantation and spontaneous epileptiform activity was recorded in 5, 7.5, and 10 mM KCl. No epileptiform activity was observed in either contralateral or ipsilateral slices from sham-implanted mice in the presence of 5 mM extracellular KCl. However, a significant proportion of ipsilateral slices from glioma-implanted mice discharged in the presence of 5 mM KCl both 1 week ($44.4 \pm 17.6\%$) and 2 weeks ($50.0 \pm 22.4\%$; $p < 0.05$ using a one-way ANOVA) post implantation. An increased percentage of contralateral slices in mice 2 weeks post glioma-implantation also exhibited epileptiform activity ($12.5 \pm 12.5\%$). Increasing the extracellular KCl concentration to 7.5 mM increases epileptiform activity in ipsilateral slices in glioma-implanted mice (1 week: $66.7 \pm 16.7\%$; 2 weeks: $100.0 \pm 0.0\%$) compared to sham ($42.9 \pm 20.0\%$). The increased epileptiform activity is restricted to the ipsilateral cortex, since there is no significant difference in the percentage of contralateral slices exhibiting epileptiform activity from sham- ($28.6 \pm 18.4\%$) or glioma-implanted (1 week: $14.3 \pm 12.6\%$; 2 weeks: $50.0 \pm 18.9\%$) mice (Fig. 3). All slices ($100.0\% \pm 0.0\%$) exhibited epileptiform activity in 10 mM KCl, which was used as control for the viability of the slices (Fig. 3; n = 5–9 slices, 3–5 mice per experimental group; $p < 0.05$ determined using a one-way ANOVA). These data demonstrate that implantation of C6 glioma cells induces peritumoral hyperexcitability and susceptibility to generate epileptiform activity consistent with previously published data from rodent models and human studies (Buckingham et al., 2011; Campbell et al., 2012; Kohling et al., 2006; Patt et al., 2000; Senner et al., 2003).

Consistent with previous reports (Campbell et al., 2012, 2015), we observe the development of spontaneous seizures in our mouse glioma model (Fig. 4a). We performed 24/7 video, EEG recording to quantify the development of spontaneous seizures. A similar number of spontaneous seizures were measured at 1 week (14.8 ± 4.0), 2 weeks (18.7 ± 2.8), and 3 weeks (11.0 ± 4.0) post glioma implantation; whereas, sham-implanted mice did not exhibit any spontaneous seizures (Fig. 4b). Glioma-implanted mice spend a progressive increased amount of time seizing (1 week: 5.4 ± 1.8 min; 2 weeks: 18.8 ± 6.6; 3 weeks: 32.3 ± 0.5 min; Fig. 4c), which is due to a progressive increase in the duration of events (1 week: 29.5

± 6.2 s; 2 weeks: 67.7 ± 18.5 s; 3 weeks: 244.9 ± 92.2 s; Fig. 4d) since the number of seizures is relatively unchanged (Fig. 4b) (n = 4 mice per experimental group; $p < 0.05$ determined using a one-way ANOVA).

3.2. KCC2 expression is reduced in the ipsliateral cortex of glioma mice

Given the role for glutamate in the regulation of KCC2 (Lee et al., 2007, 2011), we hypothesized that glutamate release from glioma cells may alter KCC2 expression in the peritumoral cortex, compromising GABAergic inhibition and contributing to the development of tumor-associated epilepsy. To test this hypothesis, Western blot analysis was performed to measure total KCC2 expression in the peritumoral cortex or sham-injected cortex two weeks following implantation. The average optical density of KCC2 expression is significantly decreased in the ipsilateral cortex of glioma-implanted mice (71.7 ± 9.4 O.D. units per 25 μg total protein) compared to contralateral cortex (106.8 ± 7.6 O.D. units per 25 μg total protein) or the ipsilateral (99.4 ± 6.6 O.D. units per 25 μg total protein) or contralateral (97.7 ± 7.6 O.D. units per 25 μg total protein) cortex of sham-implanted mice (Fig. 5b; n = 8–14 mice per experimental group; $p < 0.05$ determined using a one-way ANOVA). Since the surface expression and function of KCC2 is controlled by phosphorylation at residue Ser940 (Lee et al., 2007, 2011), we evaluated the level of phosphorylation at this site in the peritumoral cortex. Similar to total KCC2 expression, we observe a decrease in the optical density of KCC2 phosphorylation at residue Ser940 in the ipsilateral cortex of glioma-implanted mice (29.4 ± 4.7 O.D. units per 25 μg total protein) compared to contralateral cortex (45.9 ± 6.1 O.D. units per 25 μg total protein) or sham implanted mice (ipsilateral: 53.3 ± 4.9 O.D. units per 25 μg total protein; contralateral: 53.6 ± 7.2 O.D. units per 25 μg total protein) (Fig. 5*c*). Blocking glutamate release from glioma cells using an FDA approved drug that blocks system xc−, sulfasalazine (SAS) for two weeks following glioma-implantation, prevented the dephosphorylation of KCC2 residue Ser940 (ipsilateral: 62.3 ± 3.7 O.D. units per 25 μg total protein; contralateral: 62.3 ± 4.3 O.D. units per 25 μg total protein) and the downregulation of total KCC2 expression (ipsilateral: 90.8 ± 9.1 O.D. units per 25 μg total protein; contralateral: 92.2 ± 8.0 O.D. units per 25 μg total protein) (Fig. 5; n = 8–14 mice per experimental group; $p < 0.05$ determined using a one-way ANOVA). The percentage of KCC2 that is phosphorylated at residue Ser940 is significantly decreased in the ipsilateral glioma-injected cortex (27.9 ± 4.3 O.D. units per 25 μg total protein) compared to the contralateral cortex (44.0 ± 9.2 O.D. units per 25 μg total protein), sham (ipsilateral: 67.1 ± 6.6 O.D. units per 25 μg total protein; contralateral: 58.9 ± 5.9 O.D. units per 25 μg total protein), or SAS-treated animals (ipsilateral: 74.0 ± 9.6 O.D. units per 25 μg total protein; contralateral: 70.0 ± 6.4 O.D. units per 25 μg total protein) (Fig. 5d; n = 8–14 mice per experimental group; $p < 0.05$ determined using a one-way ANOVA). These data suggest that chloride homeostasis, and thus GABAergic inhibition, may be impaired in the peritumoral cortex of glioma-implanted mice. Further, these data demonstrate that glutamate release from glioma cells via system xc− plays a role in the dephosphorylation and downregulation of KCC2 in the peritumoral cortex.

3.3. GABAergic inhibition is compromised in the peritumoral region

Since KCC2 function is essential for the hyperpolarizing actions of GABA (Kaila et al., 2014), we sought to determine whether the dephosphorylation and downregulation of KCC2 alters GABAergic signaling in the peritumoral cortex. We recorded the magnitude and direction of spontaneous GABAergic postsynaptic potentials (sIPSPs) in the ipsilateral and contralateral cortex of glioma-implanted mice. Gramicidin perforated patch recordings from M1 cortical neurons in the I = 0 recording configuration demonstrated that 68.75% (11/16) of peritumoral cortical neurons had depolarizing sIPSPs compared to only 27.27% (3/11) of neurons in the contralateral cortex (Fig. 6; n = 11–16 neurons, 6–10 mice per experimental group) (χ^2 1, N = 27) = 4.49, p = 0.034). There was no difference in the resting membrane potential between neurons recorded from the different experimental groups (glioma ipsilateral: −64.7 ± 3.6 mV; glioma contralateral: −62.1 ± 5.2 mV; sham ipsilateral: −61.7 ± 5.5 mV; sham contralateral: −58.6 ± 7.2 mV). These data demonstrate that a loss of peritumoral KCC2 corresponds to a switch from hyperpolarizing to depolarizing GABAergic responses and suggests that a reduction in GABAergic inhibition may contribute to epileptiform activity in the peritumoral cortex.

3.4. A loss of KCC2 expression recapitulates the spontaneous seizure phenotype seen in the C6 glioma model

To directly investigate whether the loss of KCC2 in the peritumoral region could potentially contribute to tumor-associated epilepsy, we generated mice with a knockdown of KCC2 in the cortex similar to what we observed in the glioma mouse model. Floxed KCC2 mice were injected with AAV2-Cre-GFP into the M1 cortex (see Methods), infecting an area of the cortex similar in size to the glioma (Fig. 7a), which was sufficient to decrease KCC2 expression measured by Western blot analysis. Total KCC2 expression isolated from the ipsilateral AAV2-Cre-GFP injected cortex was decreased (56.1 ± 4.0 O.D. units per 25 μg total protein) compared to the complementary contralateral cortex (72.9 ± 1.3 O.D. units per 25 μg total protein) (Fig. 7b; n = 4; p < 0.05 determined using a Student's t-test). Injection of AAV2-Cre-GFP into floxed KCC2 mice results in a 76.9% decrease in expression (Fig. 7), comparable to the 68.7% decrease we observed in the peritumoral region in our glioma mouse model (Fig. 5). Continuous EEG recordings were performed to determine whether the loss of KCC2 was sufficient to induce spontaneous epileptiform activity. Fig. 8a shows a representative spontaneous seizure from mice with a reduction in KCC2 in the cortex (KCC2/AAV-Cre mice). The average number of events per hour were binned over the weeks post AAV2-Cre-GFP injection demonstrating a progressive increase in the number of epileptiform events (1 week: 1.6 ± 0.5, 2 weeks: 11.6 ± 4.3; 3 weeks: 15.6 ± 7.2; 4 weeks: 14.2 ± 4.4) (Fig. 8b; n = 4 mice per experimental group; p < 0.05 determined using a Student's t-test). No spontaneous epileptiform events were observed in the control, AAV-GFP injected animals (Fig. 8b). The generation of spontaneous epileptiform activity following a reduction in cortical KCC2 suggests that the glioma-induced reduction in KCC2 levels in the peritumoral cortex may contribute to the generation of tumor-associated epilepsy.

3.5. Bumetanide rescued seizure susceptibility in glioma mice

The data in this study suggests that a reduction in KCC2 and compromised GABAergic inhibition may contribute to tumor-associated seizure susceptibility. Therefore, we investigated the therapeutic potential of combating intracellular Cl^- accumulation with the NKCC1 blocker, bumetanide, on seizure susceptibility in our glioma model. Mice were implanted with subcutaneous osmotic pumps for continuous delivery of either vehicle or bumetanide at the time of glioma or sham implantation and the impact on seizure susceptibility was evaluated following kainic acid (10 mg/kg, *i.p.*) one or two weeks following glioma implantation. The latency to seizure onset was decreased in glioma mice at 1 week (2.5 ± 1.2 min) and 2 weeks (1.1 ± 0.2 min) post glioma implantation compared to sham-implanted mice (46.7 ± 23.2 min) (Fig. 9a). Bumetanide treatment increased the latency to seizure onset at 1 week (22.7 ± 19.5 min) and 2 weeks (72.4 ± 29.2 min) post glioma implantation (Fig. 9a; n = 6 mice per experimental group; $p < 0.05$ determined using a two-way ANOVA). The percent time exhibiting epileptiform activity following the onset of the first seizure episode was increased at 1 week ($93.0 \pm 1.8\%$) and 2 weeks ($92.2 \pm 2.4\%$) post glioma implantation compared to sham-implanted mice ($59.0 \pm 18.8\%$) (Fig. 9b). Bumetanide treatment decreased the percent time exhibiting epileptiform activity at 2 weeks ($37.4 \pm 22.9\%$) post glioma implantation. However, there was no statistical difference after 1 week of bumetanide treatment ($75.3 \pm 15.2\%$) compared to glioma-implanted mice or shams (Fig. 9b; n = 6 mice per experimental group; $p < 0.05$ determined using a two-way ANOVA). These data suggest that bumetanide might be a useful therapy for seizure management in tumor-associated epilepsy.

4. Discussion

This study builds on recent evidence implicating KCC2 in compromising GABAergic inhibition and, thereby, contributing to the development of tumor-associated epilepsy (Aronica et al., 2007; Campbell et al., 2015; Conti et al., 2011; Pallud et al., 2013). Here we confirm a role for KCC2 in the pathophysiology of gliomas and demonstrate that the reduction of KCC2 in the peritumoral cortex is sufficient to generate epileptiform activity. Although KCC2 agonists are underdevelopment (Gagnon et al., 2013), there are currently no KCC2 activators readily available. However, blocking chloride influx through NKCC1 with bumetanide has been shown to restore chloride homeostasis and shift the GABA reversal potential to more hyperpolarized potentials (Barmashenko et al., 2011; Cleary et al., 2013; Dzhala et al., 2008; Huberfeld et al., 2007; Tyzio et al., 2014). Here we demonstrate that restoring chloride homeostasis with bumetanide reduces glioma-associated seizure susceptibility. These data suggest that cation-chloride cotransporters may be a useful target for seizure management in patients with glial-derived brain tumors.

Targeting cation-chloride cotransporters may be useful for seizure control beyond just tumor-associated epilepsies. Altered expression of KCC2 and NKCC1 and the resulting switch from hyperpolarizing to depolarizing (and even excitatory) GABAergic signaling has been observed in experimental seizure models as well as resected tissues from patients with temporal lobe epilepsy (Campbell et al., 2015; Conti et al., 2011; Pallud et al., 2013). Treatment with bumetanide has already been shown to exert anticonvulsant effects in adult

animals (Sivakumaran and Maguire, 2016), again suggesting that bumetanide may have broad anticonvulsant effects not limited to tumor-associated epilepsy. Interestingly, recent studies suggest that a collapse in the chloride gradient resulting in excitatory actions of GABA may drive afterdischarges during the clonic phase of seizure activity (Ellender et al., 2014). This type of seizure activity is characterized by rhythmic discharges, which are reminiscent of the epileptiform activity observed following pharmacological blockade of KCC2 (Sivakumaran et al., 2015), or following knockdown of KCC2 in the cortex (Fig. 8). These data suggest that alterations in KCC2 function and excitatory actions of GABA may alter the nature of seizure activity, specifically driving repetitive discharges (Maguire, 2015). It is important to note that alterations in inhibition are not alone in driving seizure susceptibility and contributions from other neurotransmitter systems likely contribute to driving other types or are required for the more complex expression of epileptiform activity.

The observation that the knockdown of KCC2 in the cortex is sufficient to induce spontaneous seizures indicates that the down-regulation of KCC2 under pathological conditions is not likely a protective mechanism as previously proposed (Kaila et al., 2014). Downregulation of transporters, including KCC2, has been suggested to be an adaptive mechanism to protect neurons during periods of energy crisis (Kaila et al., 2014). Here we definitively demonstrate the pathological consequences of KCC2 loss which is capable of inducing spontaneous seizures. These findings further our current knowledge from a mere correlation between decreased KCC2 expression in the peritumoral cortex and tumor-associated epilepsy to a concrete demonstration that this change is capable of leading to spontaneous seizures. This is the first study to investigate the impact of a conditional knockout of KCC2 in a healthy adult mouse. Here we demonstrate that a focal loss of KCC2 in a previously healthy animal can lead to the generation of spontaneous seizures. Our lab previously demonstrated that pharmacologically blocking KCC2 in the hippocampus of healthy, wild type mice was sufficient to induce epileptiform activity (Sivakumaran et al., 2015). These findings suggest a pathophysiological role for KCC2 in the numerous studies documenting changes in the expression of chloride transporters in animal models of epilepsy and epileptogenesis (Barmashenko et al., 2011; Pathak et al., 2007). Consistent with a role for KCC2 in epilepsy, KCC2 knockout mice and heterozygous mice both exhibit spontaneous seizures (Woo et al., 2002). The evidence of spontaneous seizures in heterozygous KCC2 mice suggests that even a reduction in KCC2 may be disastrous. In fact, here we demonstrate that a partial, focal loss of KCC2 is sufficient to induce seizure activity. Thus, the pathological alterations in KCC2 expression are likely to have dire consequences. However, very little is known about the mechanisms mediating the changes in KCC2 expression under pathological conditions. Insight into the mechanisms regulating KCC2 under physiological or pathological conditions is likely to have high therapeutic significance.

Emerging evidence suggests that KCC2 is dynamically regulated (for review see (Medina et al., 2014)). Several signaling pathways have been identified which regulate KCC2 expression, including BDNF, Insulin-Like Growth Factor 1 (IGF-1), and Neurturin (for review see (Medina et al., 2014)). Good evidence exists for the role of BDNF in the activity-dependent regulation of KCC2 (for review see (Medina et al., 2014)). KCC2 is also regulated by post-translational modifications, including phosphorylation at multiple sites

(Kahle and Delpire, 2016; Kahle et al., 2013; Lee et al., 2007, 2010; Rivera et al., 2004). Relevant to the current study, the KCC2 residue Ser940 is regulated by PKC-dependent phosphorylation (Lee et al., 2007) and is dephosphorylated through a PP1-dependent mechanism (Lee et al., 2011). KCC2 expression is also regulated by direct interactions with other regulatory proteins, including the b isoform of Rac/Cdc42 guanine nucleotide exchange factor β-PIX, brain-type creatine kinase (CKB), protein associated with Myc (PAM), and Neto 2 (for more details see (Medina et al., 2014)). However, the functional impact of these protein interactions on KCC2 remains largely unknown. Further, little is known about how these interacting proteins are regulated, adding to the lack of clarity and complexity of KCC2 regulation.

Relevant to the current study, KCC2 function has been shown to be regulated by glutamatergic signaling, via NMDA receptor activation (Lee et al., 2011). The NMDA-dependent regulation of KCC2 is mediated, at least in part, by the calcium-activated protease cal-pain (Puskarjov et al., 2012). The role of Neto 2 in the regulation of KCC2 is also interesting given that Neto 2 acts as an auxillary subunit at kainate receptors. Interestingly, it was recently shown that KCC2 has direct interactions with kainate receptors (Mahadevan et al., 2014). Collectively, these findings suggest a provocative role for excitatory transmission in the regulation of KCC2, which is particularly relevant to the epilepsies.

The glutamate-mediated regulation of KCC2 is particularly relevant to brain tumor-associated epilepsies, in which many different types of tumor cells of glial origin have been shown to release excitotoxic concentrations of glutamate (Ye and Sontheimer, 1999). Preventing glutamate release from glioma cells, by blocking cystine uptake through cysteine-glutamate exchange system x_c^- with sulfasalazine (SAS), has been shown to reduce glioma progression (Chung and Sontheimer, 2009) and decrease the frequency of epileptiform events (Buckingham et al., 2011). Our hypothesis predicted that glutamate release from glioma cells mediates the dephosphorylation of Ser940 and contributes to the downregulation of KCC2 in the peritumoral cortex. This was confirmed by our data showing that in the presence of SAS dephosphorylation of Ser940 and a downregulation of KCC2 was prevented.

It is likely that the loss of KCC2 would render treatments targeting the GABAergic system ineffective, at least in the peritumoral target region. Thus, if pharmacologically blocking glutamate release through system x_c^- prevents GABAergic inhibition becoming compromised a combinatorial treatment may be effective in the treatment of tumor-associated epilepsies. Although SAS showed a poor pharmacokinetic profile, novel potent system x_c^- inhibitors are currently in development (Dixon et al., 2014). Similarly, our data demonstrate that bumetanide is effective in reducing seizures in our glioma model. These data suggest that preventing glutamate release from glioma cells or restoring GABAergic inhibition by modulating chloride homeostasis may be beneficial for the treatment of tumor-associated epilepsies. Future studies are required to elucidate the most successful strategy for treating tumor-associated epilepsies.

5. Conclusions

This study directly implicates the dephosphorylation and downregulation of KCC2 in the peritumoral region in the pathophysiology of tumor-associated epilepsy. These findings build on a body of literature implicating glutamate release from glioma cells in both tumor progression as well as in the development of tumor-associated epilepsy. The results presented here do not conflict with these important discoveries. In fact, we propose that glutamate release from glioma cells mediate the dephosphorylation and downregulation of KCC2, revealing yet another target for the treatment of tumor-associated epilepsies.

Acknowledgments

Abbreviations

GABA$_A$R	GABA$_A$ receptor
GBM	glioblastoma multiforme
KCC2	K+/Cl$^-$ co-transporter 2
KA	kainic acid
NKCC1	Na-K-Cl co-transporter 1

References

Aronica E, Boer K, Redeker S, Spliet WGM, van Rijen PC, Troost D, Gorter JA. Differential expression patterns of chloride transporters, Na+-K+-2Cl – –cotransporter and K+-Cl – –cotransporter, in epilepsy-associated malformations of cortical development. Neuroscience. 2007; 145:185–196. [PubMed: 17207578]

Barmashenko G, Hefft S, Aertsen A, Kirschstein T, Kohling R. Positive shifts of the GABAA receptor reversal potential due to altered chloride homeostasis is widespread after status epilepticus. Epilepsia. 2011; 52:1570–1578. [PubMed: 21899534]

Behrens PF, Langemann H, Strohschein R, Draeger J, Hennig J. Extracellular glutamate and other metabolites in and around RG2 rat glioma: an intracerebral microdialysis study. J Neurooncol. 2000; 47:11–22. [PubMed: 10930095]

Ben-Ari Y. Excitatory actions of gaba during development: the nature of the nurture. Nat Rev Neurosci. 2002; 3:728–739. [PubMed: 12209121]

Brandt C, Nozadze M, Heuchert N, Rattka M, Loscher W. Disease-modifying effects of phenobarbital and the NKCC1 inhibitor bumetanide in the pilocarpine model of temporal lobe epilepsy. J Neurosci. 2010; 30:8602–8612. [PubMed: 20573906]

Buckingham SC, Campbell SL, Haas BR, Montana V, Robel S, Ogunrinu T, Sontheimer H. Glutamate release by primary brain tumors induces epileptic activity. Nat Med. 2011; 17:1269–1274. [PubMed: 21909104]

Campbell SL, Buckingham SC, Sontheimer H. Human glioma cells induce hyperexcitability in cortical networks. Epilepsia. 2012; 53:1360–1370. [PubMed: 22709330]

Campbell SL, Robel S, Cuddapah VA, Robert S, Buckingham SC, Kahle KT, Sontheimer H. GABAergic disinhibition and impaired KCC2 cotransporter activity underlie tumor-associated epilepsy. Glia. 2015; 63:23–36. [PubMed: 25066727]

Castro OW, Santos VR, Pun RYK, McKlveen JM, Batie M, Holland KD, Gardner M, Garcia-Cairasco N, Herman JP, Danzer SC. Impact of corticosterone treatment on spontaneous seizure frequency and epileptiform activity in mice with chronic epilepsy. PLoS One. 2012; 7:e46044. [PubMed: 23029379]

Chung WJ, Sontheimer H. Sulfasalazine inhibits the growth of primary brain tumors independent of nuclear factor-kappaB. J Neurochem. 2009; 110:182–193. [PubMed: 19457125]

Cleary RT, Sun H, Huynh T, Manning SM, Li Y, Rotenberg A, Talos DM, Kahle KT, Jackson M, Rakhade SN, Berry G, Jensen FE. Bumetanide enhances phenobarbital efficacy in a rat model of hypoxic neonatal seizures. PLoS One. 2013; 8:e57148. [PubMed: 23536761]

Conti L, Palma E, Roseti C, Lauro C, Cipriani R, de GM, Aronica E, Limatola C. Anomalous levels of Cl(−) transporters cause a decrease of GABAergic inhibition in human peritumoral epileptic cortex. Epilepsia. 2011; 52(9):1635–1644. [PubMed: 21635237]

Dixon SJ, Patel DN, Welsch M, Skouta R, Lee ED, Hayano M, Thomas AG, Gleason CE, Tatonetti NP, Slusher BS, Stockwell BR. Pharmacological inhibition of cystine-glutamate exchange induces endoplasmic reticulum stress and ferroptosis. eLife. 2014; 3:e02523. [PubMed: 24844246]

Dzhala VI, Brumback AC, Staley KJ. Bumetanide enhances phenobarbital efficacy in a neonatal seizure model. Ann Neurol. 2008; 63:222–235. [PubMed: 17918265]

Ellender TJ, Raimondo JV, Irkle A, Lamsa KP, Akerman CJ. Excitatory effects of parvalbumin-expressing interneurons maintain hippocampal epileptiform activity via synchronous afterdischarges. J Neurosci. 2014; 34:15208–15222. [PubMed: 25392490]

Gagnon M, Bergeron MJ, Lavertu G, Castonguay A, Tripathy S, Bonin RP, Perez-Sanchez J, Boudreau D, Wang B, Dumas L, Valade I, Bachand K, Jacob-Wagner Mv, Tardif C, Kianicka I, Isenring P, Attardo G, Coull JA, De Koninck Y. Chloride extrusion enhancers as novel therapeutics for neurological diseases. Nat Med. 2013; 19:1524–1528. [PubMed: 24097188]

Hewitt SA, Wamsteeker JI, Kurz EU, Bains JS. Altered chloride homeostasis removes synaptic inhibitory constraint of the stress axis. Nat Neurosci. 2009; 12:438–443. [PubMed: 19252497]

Huberfeld G, Wittner L, Clemenceau S, Baulac M, Kaila K, Miles R, Rivera C. Perturbed chloride homeostasis and GABAergic signaling in human temporal lobe epilepsy. J Neurosci. 2007; 27:9866–9873. [PubMed: 17855601]

Iuchi T, Hasegawa Y, Kawasaki K, Sakaida T. Epilepsy in patients with gliomas: Incidence and control of seizures. J Clin Neurosci. 2015; 22:87–91. [PubMed: 25192590]

Kahle KT, Delpire E. Kinase-KCC2 coupling: Cl– rheostasis, disease susceptibility, therapeutic target. J Neurophysiol. 2016; 115:8–18. [PubMed: 26510764]

Kahle KT, Staley KJ, Nahed BV, Gamba G, Hebert SC, Lifton RP, Mount DB. Roles of the cation-chloride cotransporters in neurological disease. Nat Clin Pract Neurol. 2008; 4:490–503. [PubMed: 18769373]

Kahle KT, Deeb TZ, Puskarjov M, Silayeva L, Liang B, Kaila K, Moss SJ. Modulation of neuronal activity by phosphorylation of the K–Cl cotransporter KCC2. Trends Neurosci. 2013; 36:726–737. [PubMed: 24139641]

Kaila K, Ruusuvuori E, Seja P, Voipio J, Puskarjov M. GABA actions and ionic plasticity in epilepsy. Curr Opin Neurobiol. 2014; 26:34–41. [PubMed: 24650502]

Kerkhof M, Vecht CJ. Seizure characteristics and prognostic factors of gliomas. Epilepsia. 2013; 54:12–17. [PubMed: 24328866]

Kohling R, Senner V, Paulus W, Speckmann EJ. Epileptiform activity preferentially arises outside tumor invasion zone in glioma xenotransplants. Neurobiol Dis. 2006; 22:64–75. [PubMed: 16309916]

Lee V, Maguire J. Impact of inhibitory constraint of interneurons on neuronal excitability. J Neurophysiol. 2013; 110(11):2520–2535. [PubMed: 24027099]

Lee HH, Walker JA, Williams JR, Goodier RJ, Payne JA, Moss SJ. Direct protein kinase C-dependent phosphorylation regulates the cell surface stability and activity of the potassium chloride cotransporter KCC2. J Biol Chem. 2007; 282:29777–29784. [PubMed: 17693402]

Lee HH, Jurd R, Moss SJ. Tyrosine phosphorylation regulates the membrane trafficking of the potassium chloride co-transporter KCC2. Mol Cell Neurosci. 2010; 45:173–179. [PubMed: 20600929]

Lee HH, Deeb TZ, Walker JA, Davies PA, Moss SJ. NMDA receptor activity downregulates KCC2 resulting in depolarizing GABA(A) receptor-mediated currents. Nat Neurosci. 2011; 14:736–743. [PubMed: 21532577]

MacKenzie G, Maguire J. Chronic stress shifts the GABA reversal potential in the hippocampus and increases seizure susceptibility. Epilepsy Res. 2015; 109:13–27. [PubMed: 25524838]

Maguire JL. Implicating interneurons: optogenetic studies suggest that interneurons are guilty of contributing to epileptiform activity. Epilepsy Curr. 2015; 15:213–216. [PubMed: 26316871]

Mahadevan V, Pressey J, Acton B, Uvarov P, Huang M, Chevrier J, Puchalski A, Li C, Ivakine E, Airaksinen M, Delpire E, McInnes R, Woodin M. Kainate receptors coexist in a functional complex with KCC2 and regulate chloride homeostasis in hippocampal neurons. Cell Rep. 2014; 7:1762–1770. [PubMed: 24910435]

Marcus HJ, Carpenter KLH, Price SJ, Hutchinson PJ. In vivo assessment of high-grade glioma biochemistry using microdialysis: a study of energy-related molecules, growth factors and cytokines. J Neurooncol. 2009; 97:11–23. [PubMed: 19714445]

Medina I, Friedel P, Rivera C, Kahle KT, Kourdougli N, Uvarov P, Pellegrino C. Current view on the functional regulation of the neuronal K(+)-Cl-cotransporter KCC2. Front Cell Neurosci. 2014; 8:27. [PubMed: 24567703]

O'Toole KK, Hooper A, Wakefield S, Maguire J. Seizure-induced disinhibition of the HPA axis increases seizure susceptibility. Epilepsy Res. 2013; 108(1):29–43. [PubMed: 24225328]

Pallud J, Capelle L, Huberfeld G. Tumoral epileptogenicity: how does it happen? Epilepsia. 2013; 54:30–34.

Pathak HR, Weissinger F, Terunuma M, Carlson GC, Hsu FC, Moss SJ, Coulter DA. Disrupted dentate granule cell chloride regulation enhances synaptic excitability during development of temporal lobe epilepsy. J Neurosci. 2007; 27:14012–14022. [PubMed: 18094240]

Patt S, Steenbeck J, Hochstetter A, Kraft R, Huonker R, Haueisen J, Haberland N, Ebmeier K, Hliscs R, Fiehler J, Nowak H, Kalff R. Source localization and possible causes of interictal epileptic activity in tumor-associated epilepsy. Neurobiol Dis. 2000; 7:260–269. [PubMed: 10964598]

Payne JA, Rivera C, Voipio J, Kaila K. Cation-chloride co-transporters in neuronal communication, development and trauma. Trends Neurosci. 2003; 26:199–206. [PubMed: 12689771]

Puskarjov M, Ahmad F, Kaila K, Blaesse P. Activity-dependent cleavage of the K-Cl cotransporter KCC2 mediated by calcium-activated protease calpain. J Neurosci. 2012; 32:11356–11364. [PubMed: 22895718]

Rivera C, Voipio J, Payne JA, Ruusuvuori E, Lahtinen H, Lamsa K, Pirvola U, Saarma M, Kaila K. The K+/Cl− co-transporter KCC2 renders GABA hyperpolarizing during neuronal maturation. Nature. 1999; 397:251–255. [PubMed: 9930699]

Rivera C, Voipio J, Thomas-Crusells J, Li H, Emri Z, Sipila S, Payne JA, Minichiello L, Saarma M, Kaila K. Mechanism of activity-dependent downregulation of the neuron-specific K-Cl cotransporter KCC2. J Neurosci. 2004; 24:4683–4691. [PubMed: 15140939]

Sarkar J, Wakefield S, Mackenzie G, Moss SJ, Maguire J. Neurosteroidogenesis is required for the physiological response to stress: role of neurosteroid-Sensitive GABAA receptors. J Neurosci. 2011; 31:18198–18210. [PubMed: 22171026]

Senner V, Kohling R, Puttmann-Cyrus S, Straub H, Paulus W, Speckmann EJ. A new neurophysiological/neuropathological ex vivo model localizes the origin of glioma-associated epileptogenesis in the invasion area. Acta Neuropathol (Berl). 2003; 107:1–7. [PubMed: 13680280]

Silayeva L, Deeb TZ, Hines RM, Kelley MR, Munoz MB, Lee HHC, Brandon NJ, Dunlop J, Maguire J, Davies PA, Moss SJ. KCC2 activity is critical in limiting the onset and severity of status epilepticus. Proc Natl Acad Sci U S A. 2015; 112:3523–3528. [PubMed: 25733865]

Sivakumaran S, Maguire J. Bumetanide reduces seizure progression and the development of pharmacoresistant status epilepticus. Epilepsia. 2016; 57:222–232. [PubMed: 26659482]

Author Manuscript

Author Manuscript

Author Manuscript

Author Manuscript

Sivakumaran S, Cardarelli RA, Maguire J, Kelley MR, Silayeva L, Morrow DH, Mukherjee J, Moore YE, Mather RJ, Duggan ME, Brandon NJ, Dunlop J, Zicha S, Moss SJ, Deeb TZ. Selective inhibition of KCC2 leads to hyperexcitability and epileptiform discharges in hippocampal slices and In vivo. J Neurosci. 2015; 35:8291–8296. [PubMed: 26019342]

Tyzio R, Nardou R, Ferrari DC, Tsintsadze T, Shahrokhi A, Eftekhari S, Khalilov I, Tsintsadze V, Brouchoud C, Chazal G, Lemonnier E, Lozovaya N, Burnashev N, Ben-Ari Y. Oxytocin-Mediated GABA inhibition during delivery attenuates autism pathogenesis in rodent offspring. Science. 2014; 343:675–679. [PubMed: 24503856]

Woo NS, Lu J, England R, McClellan R, Dufour S, Mount DB, Deutch AY, Lovinger DM, Delpire E. Hyperexcitability and epilepsy associated with disruption of the mouse neuronal-specific K–Cl cotransporter gene. Hippocampus. 2002; 12:258–268. [PubMed: 12000122]

Ye ZC, Sontheimer H. Glioma cells release excitotoxic concentrations of glutamate. Cancer Res. 1999; 59:4383–4391. [PubMed: 10485487]

Ye ZC, Rothstein JD, Sontheimer H. Compromised glutamate transport in human glioma cells: reduction-mislocalization of sodium-dependent glutamate transporters and enhanced activity of cystine-glutamate exchange. J Neurosci. 1999; 19:10767–10777. [PubMed: 10594060]

Yu J, Proddutur A, Elgammal FS, Ito T, Santhakumar V. Status epilepticus enhances tonic GABA currents and depolarizes GABA reversal potential in dentate fast-spiking basket cells. J Neurophysiol. 2013; 109:1746–1763. [PubMed: 23324316]

Yuen TI, Morokoff AP, Bjorksten A, D'Abaco G, Paradiso L, Finch S, Wong D, Reid CA, Powell KL, Drummond KJ, Rosenthal MA, Kaye AH, O'Brien TJ. Glutamate is associated with a higher risk of seizures in patients with gliomas. Neurology. 2012; 79:883–889. [PubMed: 22843268]

de Groot J, Sontheimer H. Glutamate and the biology of gliomas. Glia. 2011; 59:1181–1189. [PubMed: 21192095]

de Groot JF, Liu TJ, Fuller G, Yung WKA. The excitatory amino acid transporter-2 induces apoptosis and decreases glioma growth in vitro and In vivo. Cancer Res. 2005; 65:1934–1940. [PubMed: 15753393]

de Groot M, Reijneveld JC, Aronica E, Heimans JJ. Epilepsy in patients with a brain tumour: focal epilepsy requires focused treatment. Brain. 2012; 135:1002–1016. [PubMed: 22171351]

van Breemen MS, Wilms EB, Vecht CJ. Epilepsy in patients with brain tumours: epidemiology, mechanisms, and management. Lancet Neurol. 2007; 6:421–430. [PubMed: 17434097]

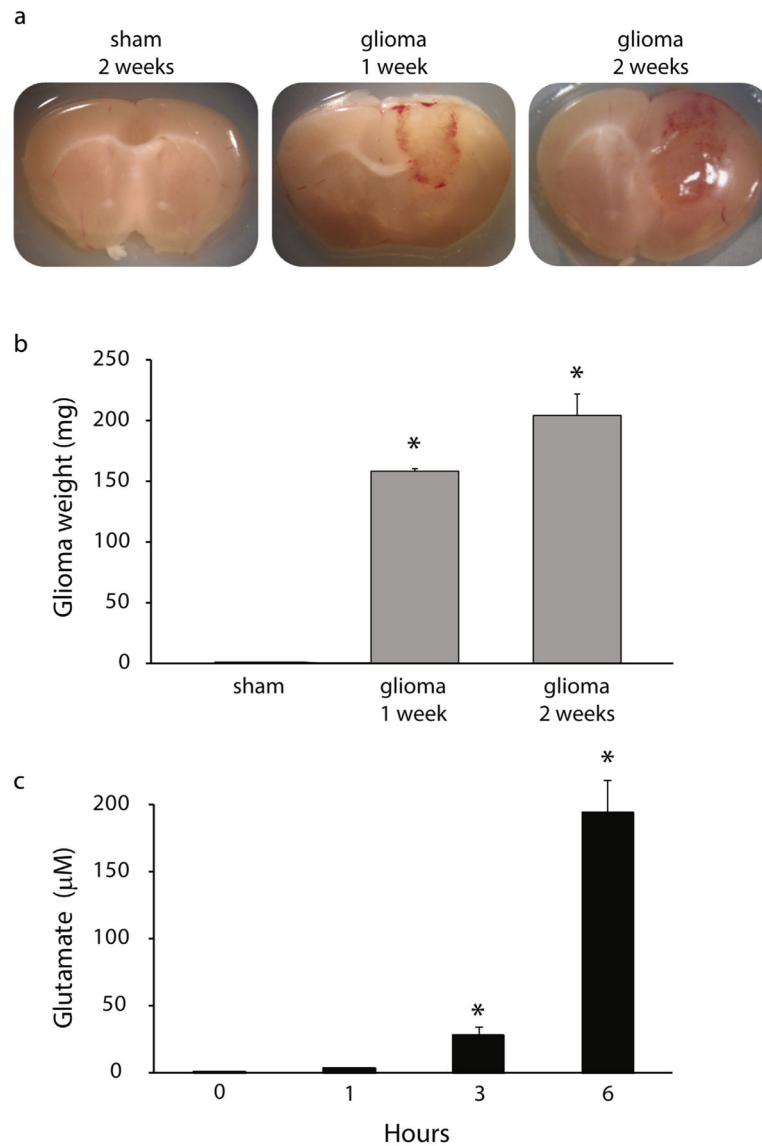**Fig. 1.**
Tumor progression in a mouse glioma model.

(a) Representative images of coronal sections through the brain of sham- implanted mice and glioma-implanted mice 1 and 2 weeks post implantation. (b) The average weight of the tumor mass excised from mice at 1 and 2 weeks post glioma-implantation. n = 6 mice per experimental group. *Denotes a p value < 0.05 using a one-way ANOVA. (c) Average glutamate concentrations measured in cultures of C6 glioma cells at 0, 1, 3, and 6 h. n = 4 per experimental group. *Denotes a p value <0.05 using a repeated measures ANOVA.
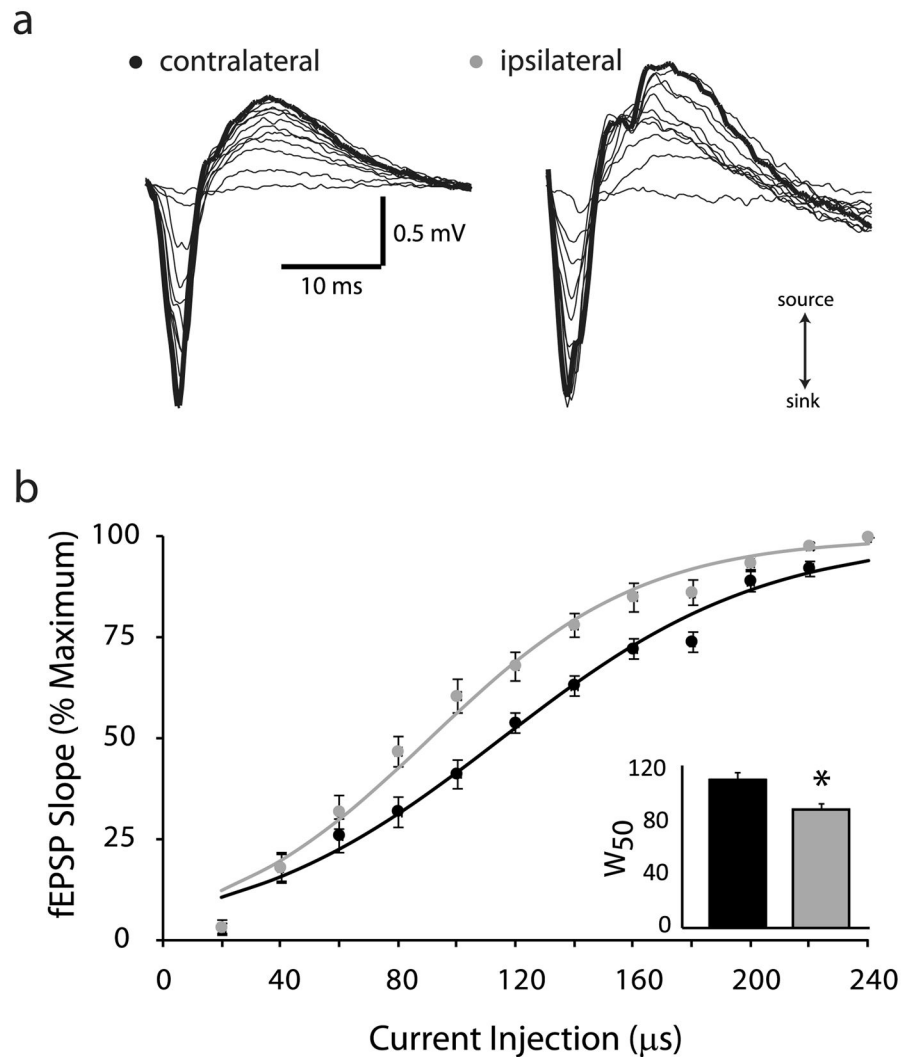
Fig. 2.
Glioma-induced increase in network excitability.

(a) Representative fEPSPs in response to a threshold stimulation intensity and increasing stimulation widths from 20 μs–240 μs in the glioma-injected ipsilateral and contralateral cortices. The slope of the fEPSP was calculated over an area indicated with a grey bar on the rising phase of the fEPSP corresponding to the source (upward slope). (b) The percent maximum fEPSP slope is plotted against the stimulation width to generate input-output curves from the ipsilateral (grey dots) and contralateral (black dots) cortices. The input-output curves were fit with a Boltzmann function which demonstrates a leftward shift in the input-output curve from the ipsilateral cortex (grey line) compared to the contralateral cortex (black line). inset, The half maximum stimulation width (W_{50}), calculated from the Boltzmann fits, was decreased in the ipsilateral cortex (grey bars) compared to the contralateral cortex (black bars). n = 10 slices, 3–4 mice per experimental group. *Denotes a p value <0.05 determined using a Student's t-test.
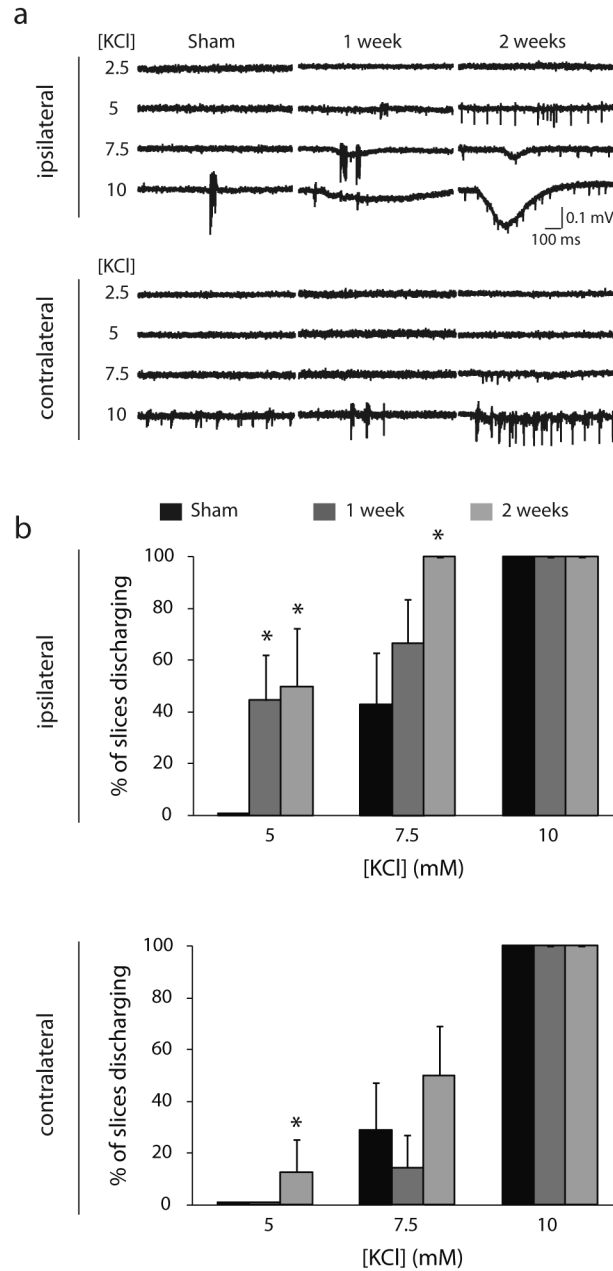
Fig. 3.
Increased susceptibility for epileptiform activity in glioma-implanted mice.
(a) Representative traces of epileptiform activity in the ipsilateral (top traces) or contralateral cortices (bottom traces) of sham- and glioma-implanted mice generated in the presence of 5, 7.5, or 10 mM KCl at 1 week or 2 weeks post implantation. (b) The percentage of slices discharging in the ipsilateral cortex (top histogram) or contralateral cortex (bottom histogram) in the presence of 5, 7.5, or 10 mM KCl in sham (black bars) or glioma-implanted mice at 1 week (dark grey bars) or 2 weeks post implantation (light grey bars). n = 5–9 slices, 3–5 mice per experimental group. *Denotes a p value <0.05 determined using a one-way ANOVA.
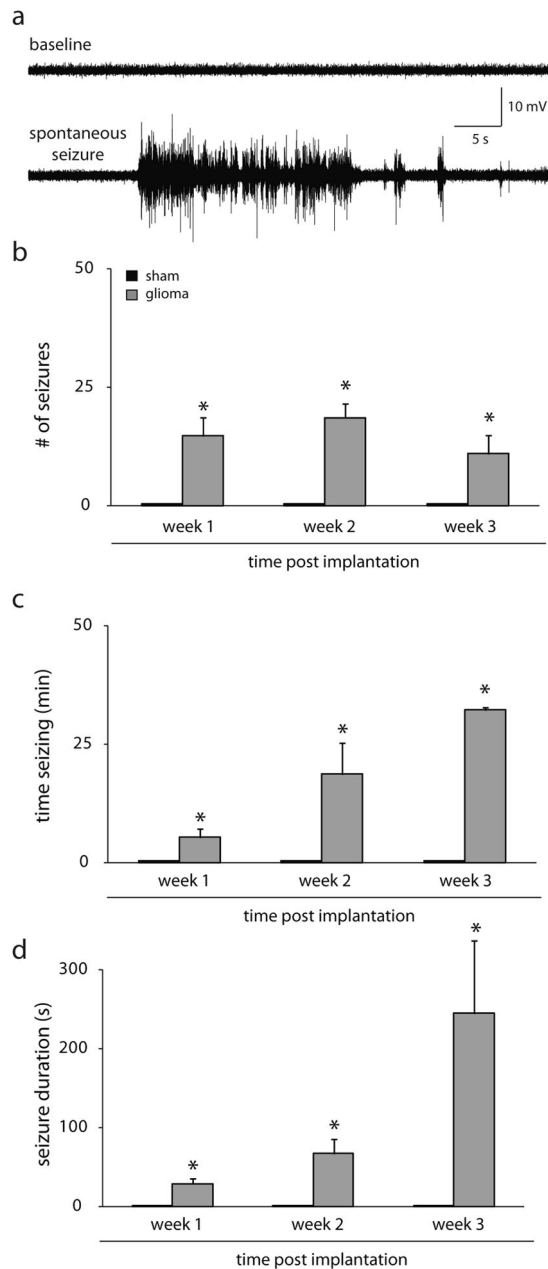
Fig. 4.

Spontaneous seizures in the mouse glioma model.

(a) Representative traces of baseline EEG activity and a spontaneous seizure recorded from a glioma-implanted mouse. (b) The average number of spontaneous seizures observed in sham- (black bars) and glioma- (grey bars) implanted mice at 1–3 weeks post implantation. No spontaneous seizures observed in sham-implanted mice; whereas, spontaneous seizures were observed in glioma-implanted mice. The amount of time seizing per day (c) and the average duration of epileptiform events (d) increased over time post glioma-implantation. n = 4 mice per experimental group. *Denotes a p value <0.05 determined using a one-way ANOVA.
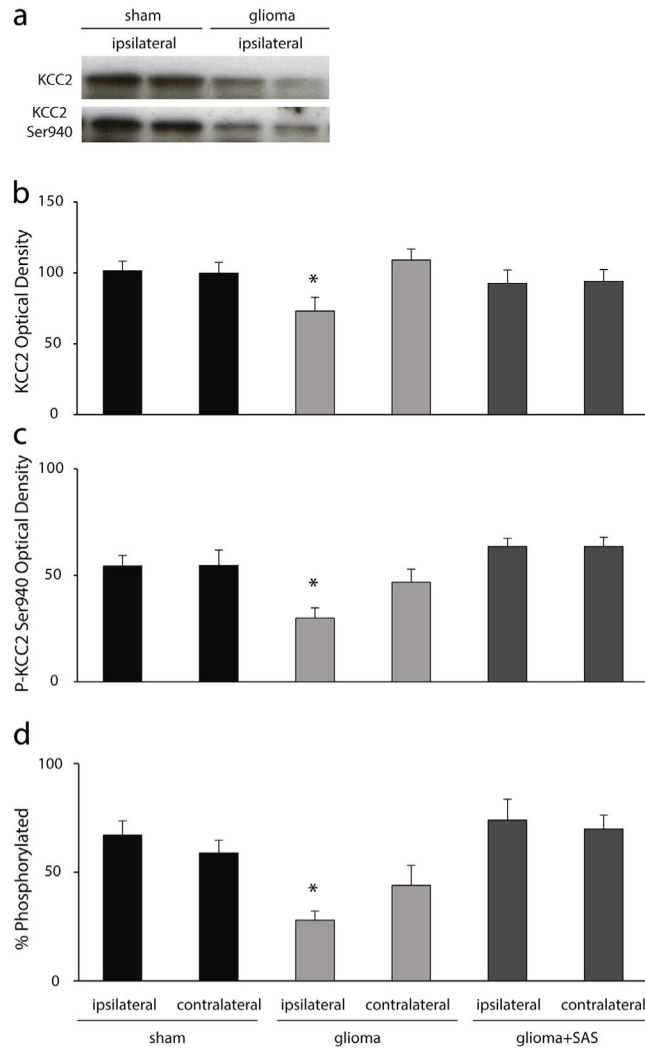
Fig. 5.
Dephosphorylation and downregulation of KCC2 in glioma-implanted mice.
(a) Representative Western blots of total KCC2 expression and the phosphorylation of KCC2 (P-KCC2) at residue Ser940 in total protein isolated from the ipsilateral cortex of two independent sham- or glioma-implanted mice. (b) The average optical density total KCC2 levels is decreased in the ipsilateral cortex of glioma-implanted mice compared levels measured in the contralateral cortex or in sham-implanted mice. Treatment with SAS prevented the downregulation of KCC2 in the ipsilateral glioma-implanted cortex. (c) The phosphorylation of KCC2 at residue Ser940 is decreased in the ipsilateral cortex of glioma-implanted mice compared to the contralateral cortex or sham-implanted mice. Treatment with SAS prevented the dephosphorylation of KCC2 at residue Ser940 in the ipsilateral glioma-implanted cortex. (d) The percent of KCC2 that is phosphorylated at residue Ser940 is not statistically different between experimental groups. n = 4–7 per experimental group. *Denotes a *p* value <0.05 determined using a one-way ANOVA.
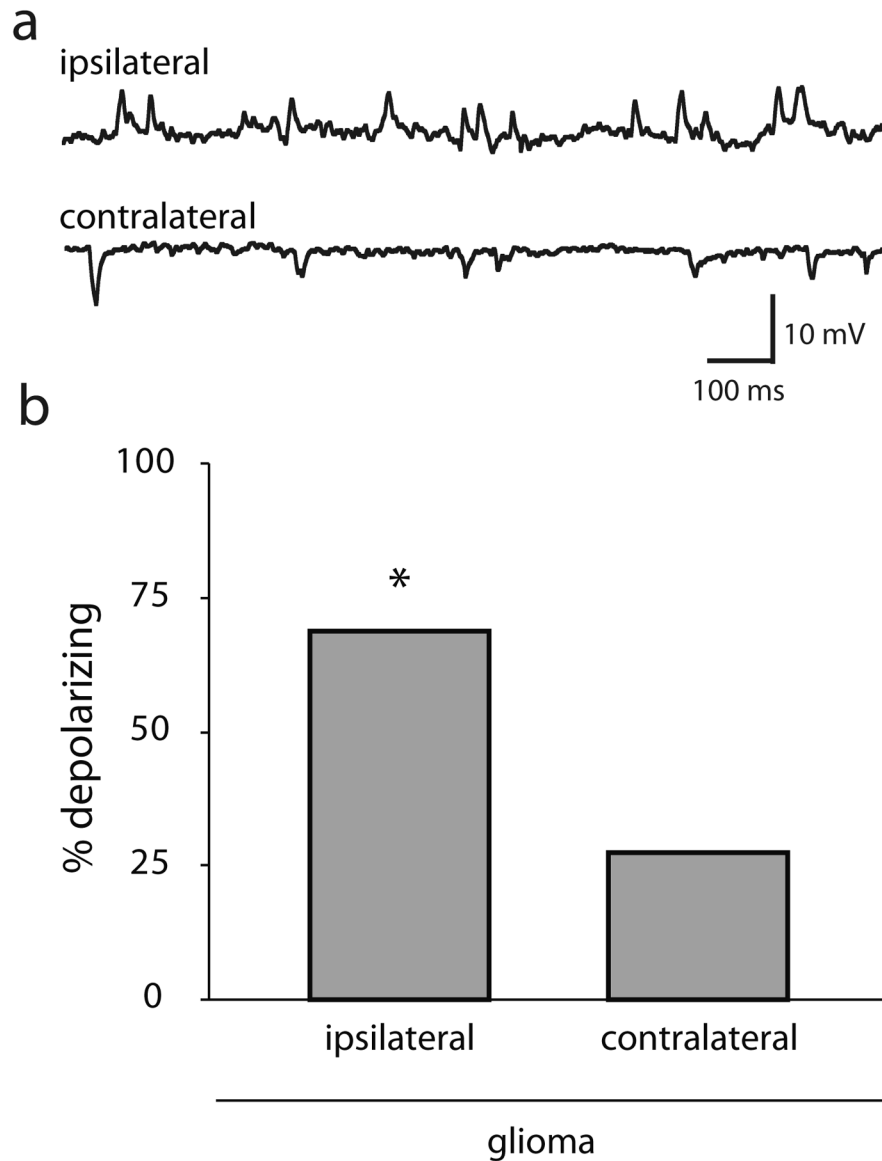
Fig. 6.
Depolarizing GABAergic signaling in the glioma-implanted mice.
(a) Representative traces of depolarizing GABAergic postsynaptic potentials in the peritumoral cortex of glioma-implanted mice in contrast to hyperpolarizing IPSPs in the contralateral cortex. (b) The percentage of neurons with depolarizing GABAergic postsynaptic potentials is increased in the ipsilateral cortex compared to the contralateral cortex where the majority of IPSPs are hyperpolarizing. n = 11–16 neurons, 6–10 mice per experimental group. *Denotes a p value <0.05 determined using a χ^2 test.
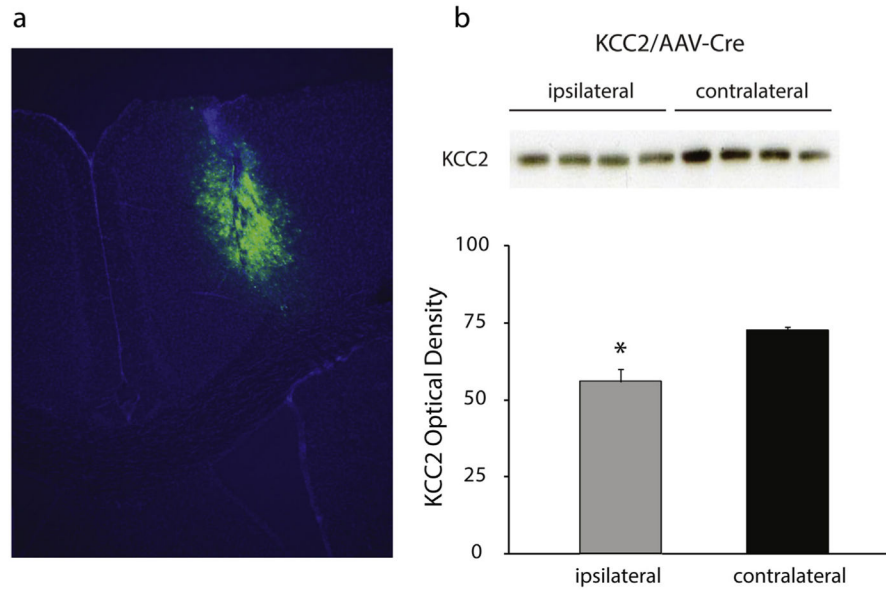
Fig. 7.
Focal knockdown of KCC2 in the cortex.

(a) A representative image showing the extent of AAV2-Cre-GFP expression in the cortex of floxed KCC2 mice. (b) Representative Western blots of total KCC2 expression in total protein isolated from the ipsilateral and contralateral cortices of KCC2/AAV-Cre mice. The average optical density of total KCC2 expression is decreased in the ipsilateral cortex of KCC2/AAV-Cre mice compared to the contralateral cortex. n = 4 per experimental group. *Denotes a p value <0.05 determined using a Student's t-test.
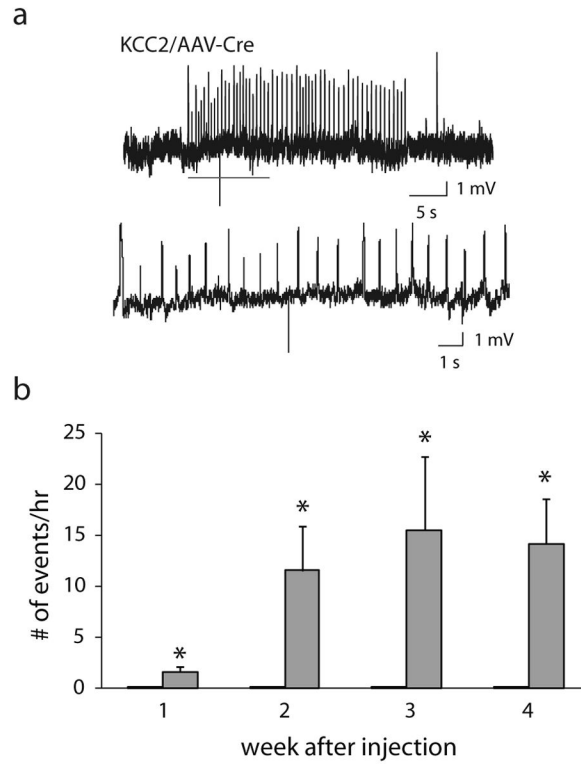
Fig. 8.
Spontaneous epileptiform activity in KCC2/AAV-Cre mice.

(a) Representative traces of spontaneous epileptiform activity recorded from KCC2/AAV-Cre mice. The higher magnification traces highlight the abnormal, rhythmic epileptiform activity. (b) Quantification of the number of spontaneous epileptiform events per hour recorded in KCC2/AAV-Cre mice (grey bars), which were never observed in control, AAV-GFP injected mice (black bars). n = 4 mice per experimental group. *Denotes a *p* value <0.05 determined using a Student's *t*-test.
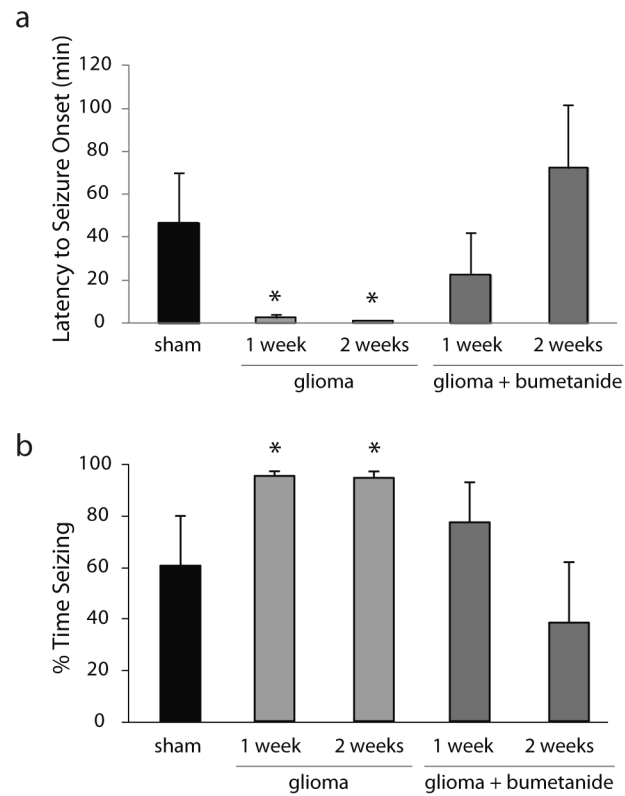
a

b

Fig. 9.
Bumetanide decreases seizure susceptibility in glioma-implanted mice.

The latency to seizure onset (a) and the percent time exhibiting epileptiform activity (b) for two hours following kainic acid (10 mg/kg) administration in vehicle and bumetanide-treated mice implanted with a glioma two weeks prior compared to sham-implanted mice. n = 6 mice per experimental group. * Denotes a p value < 0.05 determined using a two-way ANOVA.